Quantum Simulation of Light-Matter Interaction

Breaking the Rotating Wave Approximation in the Deep Strong Coupling Regime

HE 381 Term Paper

Team Members:
1. Ankush Kumar (SR No.: 24033)
2. Suman Dafadar (SR No.: 24139)

Instructor: Prof. Aninda Sinha

November 30, 2025

Contents

1 Introduction

The quantum mechanical interaction between a two-level system (an "atom" or qubit) and a quantized harmonic oscillator (a "cavity" or bosonic mode) is the fundamental building block of quantum optics. This paradigmatic system describes a wide array of physical phenomena, from the spontaneous emission of an atom in free space to the coherent manipulation of superconducting qubits in a dilution refrigerator.

Historically, this interaction has been studied in the weak or strong coupling regimes, where the coupling rate g is significantly smaller than the atomic transition frequency ω_a and the cavity frequency ω_c. In these regimes, the system's dynamics are accurately described by the Jaynes-Cummings (JC) model [1], first proposed in 1963. The JC model relies on the Rotating Wave Approximation (RWA), a mathematical simplification that neglects rapidly oscillating terms in the interaction Hamiltonian. This approximation is valid when the interaction timescale ($1/g$) is much slower than the oscillation period of the light ($1/\omega$), allowing the fast terms to average out to zero. The JC model predicts the conservation of the total number of excitations in the system, leading to intuitive phenomena such as vacuum Rabi oscillations where energy is coherently swapped between the atom and the field.

However, the landscape of quantum technology has evolved dramatically. Platforms such as circuit quantum electrodynamics (cQED) [3] and trapped ions [5] now allow for coupling strengths that rival or even exceed the system frequencies ($g \gtrsim \omega$). This is known as the **Ultrastrong** and **Deep Strong Coupling (DSC)** regime. In this extreme regime, the assumptions underlying the RWA break down. The counter-rotating terms—processes where an atom is excited while creating a photon, or relaxes while destroying one—become significant. This leads to a violation of the conservation of excitation number and introduces complex, non-perturbative physics.

The physical consequences of the breakdown of the RWA are profound. The ground state of the system is no longer the empty vacuum $|g, 0\rangle$, but rather a complex, entangled state containing a finite population of "virtual" photons. This interaction with the vacuum fluctuations leads to the **Bloch-Siegert shift**, a correction to the energy spectrum analogous to the Lamb shift in atomic physics. Furthermore, the dynamics of the system become chaotic, exhibiting **collapse-and-revival** phenomena as the atomic state becomes entangled with a multi-photon wavepacket.

Simulating these regimes is computationally demanding for classical computers as the Hilbert space grows exponentially with the number of modes. Quantum computers offer a natural platform for such simulations. By mapping the bosonic and atomic degrees of freedom onto qubits, we can explore the dynamics of the full Quantum Rabi Model (QRM) directly, bypassing the limitations of classical approximations.

In this term paper, we present a comprehensive study of the transition from the JC model to the QRM. We employ a hybrid approach, combining classical exact diagonalization benchmarks with digital quantum simulation on IBM Quantum hardware. Our specific objectives are:

1. To theoretically derive and numerically compute the discrete energy spectrum of the JC and Rabi models, identifying the **Bloch-Siegert shift**.

2. To investigate the time evolution of the system, distinguishing between standard Rabi oscillations and the **collapse-and-revival** dynamics unique to the DSC regime.

3. To implement the simulation on a quantum computer using the **Variational Quantum Eigensolver (VQE)** for spectral analysis and **Trotterization** for dynamical evolution.

4. To execute the simulation on real hardware (**IBM Torino**), analyzing the impact of device noise and validating our results against a custom noise model.

2 Theoretical Framework

2.1 The Quantum Rabi Hamiltonian

The most general description of a two-level system coupled to a single bosonic mode is given by the Quantum Rabi Hamiltonian. Setting $\hbar = 1$, it is written as:

$$H_{Rabi} = H_{field} + H_{atom} + H_{interaction} \tag{1}$$

$$H_{Rabi} = \omega_c \hat{a}^\dagger \hat{a} + \frac{\omega_a}{2}\hat{\sigma}_z + g\hat{\sigma}_x(\hat{a}^\dagger + \hat{a}) \tag{2}$$

Here:

- ω_c is the frequency of the cavity mode.
- ω_a is the transition frequency of the two-level system.
- g is the coupling strength between the atom and the field.
- $\hat{a}^\dagger, \hat{a}$ are the creation and annihilation operators for the field, satisfying the commutation relation $[\hat{a}, \hat{a}^\dagger] = 1$.
- $\hat{\sigma}_z, \hat{\sigma}_x$ are the Pauli spin operators for the atom, satisfying $[\hat{\sigma}_i, \hat{\sigma}_j] = 2i\epsilon_{ijk}\hat{\sigma}_k$.

The interaction term $g\hat{\sigma}_x(\hat{a}^\dagger + \hat{a})$ represents the dipole coupling. Using the ladder operators $\hat{\sigma}_x = \hat{\sigma}_+ + \hat{\sigma}_-$, we can expand this product:

$$H_{int} = g(\hat{\sigma}_+ + \hat{\sigma}_-)(\hat{a}^\dagger + \hat{a}) = g(\hat{\sigma}_+\hat{a} + \hat{\sigma}_-\hat{a}^\dagger) + g(\hat{\sigma}_+\hat{a}^\dagger + \hat{\sigma}_-\hat{a}) \tag{3}$$

2.1.1 Energy Conserving (Co-Rotating) Terms

The first group, $g(\hat{\sigma}_+\hat{a}+\hat{\sigma}_-\hat{a}^\dagger)$, describes resonant energy exchange processes where energy is conserved (in the absence of detuning).

- $\hat{\sigma}_+\hat{a}$: The atom absorbs a photon ($\hat{a}$) and transitions from ground to excited state ($\hat{\sigma}_+$). Total energy change: $\omega_a - \omega_c \approx 0$.
- $\hat{\sigma}_-\hat{a}^\dagger$: The atom emits a photon ($\hat{a}^\dagger$) and transitions from excited to ground state ($\hat{\sigma}_-$). Total energy change: $\omega_c - \omega_a \approx 0$.

These processes conserve the total excitation number operator:

$$\hat{N} = \hat{a}^\dagger\hat{a} + \hat{\sigma}_+\hat{\sigma}_- \tag{4}$$

2.1.2 Counter-Rotating Terms

The second group, $g(\hat{\sigma}_+\hat{a}^\dagger + \hat{\sigma}_-\hat{a})$, describes "virtual" processes that seemingly violate energy conservation.

- $\hat{\sigma}_+\hat{a}^\dagger$: The atom becomes excited AND a photon is created. Total energy change: $\omega_a + \omega_c$.
- $\hat{\sigma}_-\hat{a}$: The atom relaxes AND a photon is destroyed. Total energy change: $-(\omega_a + \omega_c)$.

In the Interaction Picture, these terms oscillate at the sum frequency $\omega_a + \omega_c$. When $g \ll (\omega_a + \omega_c)$, these terms oscillate rapidly and average to zero over any significant timescale. This justifies neglecting them, which is the essence of the **Rotating Wave Approximation (RWA)**.

2.2 The Jaynes-Cummings Model

Applying the RWA yields the Jaynes-Cummings Hamiltonian:

$$H_{JC} = \omega_c\hat{a}^\dagger\hat{a} + \frac{\omega_a}{2}\hat{\sigma}_z + g(\hat{\sigma}_+\hat{a} + \hat{\sigma}_-\hat{a}^\dagger) \tag{5}$$

Because $[\hat{H}_{JC}, \hat{N}] = 0$, the Hamiltonian connects only states with the same number of excitations (e.g., $|e, n\rangle$ and $|g, n+1\rangle$). This block-diagonal structure allows for analytical solution. The eigenstates are the famous "dressed states" $|n, \pm\rangle$:

$$E_{n,\pm} = n\omega_c \pm \frac{1}{2}\sqrt{(\omega_a - \omega_c)^2 + 4g^2(n+1)} \tag{6}$$

This linear dependence on $\sqrt{n}$ leads to the characteristic Rabi splitting observed in vacuum ($\sqrt{1}$) and with photons ($\sqrt{n+1}$).

2.3 Deep Strong Coupling & The Bloch-Siegert Shift

In the Deep Strong Coupling regime ($g \approx \omega$), the RWA is invalid. The counter-rotating terms are no longer negligible perturbations; they are as strong as the system's natural frequency. They couple states with different excitation numbers (e.g., coupling $|g, 0\rangle \leftrightarrow |e, 1\rangle \leftrightarrow |g, 2\rangle$).

This leads to three major physical consequences:

2.3.1 1. Vacuum Entanglement

In the JC model, the ground state is the simple product state $|g, 0\rangle$. In the QRM, the counter-rotating terms mix this state with higher excitation states (like $|e, 1\rangle$, $|g, 2\rangle$, etc.). The true ground state $|G\rangle$ becomes an entangled state:

$$|G\rangle = c_0|g, 0\rangle + c_1|e, 1\rangle + c_2|g, 2\rangle + \dots \tag{7}$$

This means the vacuum contains a finite population of photons, even in the ground state. The atom is "dressed" by these virtual vacuum fluctuations.

2.3.2 2. The Bloch-Siegert Shift

The interaction with these virtual photons lowers the energy of the ground state. While the JC model predicts a constant ground state energy of $-\omega_a/2$, the QRM predicts a shift dependent on g^2. This correction is known as the **Bloch-Siegert shift**.

$$\Delta E_{BS} \approx \frac{g^2}{\omega_a + \omega_c} \tag{8}$$

This shift is a clear spectral signature of the breakdown of the RWA.

2.3.3 3. Parity Symmetry

Although $\hat{N}$ is not conserved, the QRM possesses a discrete $\mathbb{Z}_2$ parity symmetry defined by the operator:

$$\hat{\Pi} = -\hat{\sigma}_z(-1)^{\hat{a}^\dagger \hat{a}} = e^{i\pi \hat{N}} \tag{9}$$

The Hamiltonian commutes with this parity operator, $[\hat{H}_{Rabi}, \hat{\Pi}] = 0$. This splits the Hilbert space into two independent chains (even and odd parity). The dynamics are constrained to these chains, leading to the interference effects that cause the collapse-and-revival of Rabi oscillations.

3 Methodology

3.1 Exact Diagonalization (Classical Benchmark)

Before running quantum simulations, we established a "ground truth" using classical numerical methods. We truncated the infinite Hilbert space of the cavity to $N = 20$ Fock states. This results in a Hamiltonian matrix of size $2N \times 2N = 40 \times 40$.

We used Python (`NumPy`) to construct the matrix representations of the operators in the basis $\{|g,0\rangle, |e,0\rangle, |g,1\rangle, |e,1\rangle, \dots\}$. For example, the annihilation operator for $N = 3$ looks like:

$$\hat{a} = \begin{pmatrix} 0 & \sqrt{1} & 0 \\ 0 & 0 & \sqrt{2} \\ 0 & 0 & 0 \end{pmatrix} \tag{10}$$

We diagonalized H_{JC} and H_{Rabi} to obtain the eigenvalues (energy spectrum) as a function of g. We then computed the time evolution unitary $U(t) = e^{-iHt}$ and applied it to an initial excited state $|\psi(0)\rangle = |e,0\rangle$ to track the expectation value $\langle \hat{\sigma}_z(t) \rangle$.

3.2 Digital Quantum Simulation on Qiskit

To simulate this physics on a gate-based quantum computer, we mapped the bosonic and atomic degrees of freedom onto qubits using the `Qiskit` SDK.

3.2.1 Qubit Mapping Strategy

The atom is naturally represented by a single qubit. The cavity, however, requires a mapping strategy. We used a binary encoding where the first N Fock states are mapped to $k = \lceil \log_2 N \rceil$ qubits.

- **Atom:** 1 Qubit. State $|g\rangle \to |0\rangle$, $|e\rangle \to |1\rangle$.
- **Cavity (Truncation):**
  - For **High-Fidelity Simulations** (Local Simulator): We used $N = 32$ levels, requiring 5 cavity qubits + 1 atom qubit = 6 qubits total.
  - For **Hardware Execution** (IBM Torino): To minimize decoherence and circuit depth, we used a truncated model with $N = 2$ levels, requiring 1 cavity qubit + 1 atom qubit = 2 qubits total.

3.2.2 Algorithm 1: Variational Quantum Eigensolver (VQE)

We employed VQE to determine the ground state energy. VQE is a hybrid quantum-classical algorithm suitable for Noisy Intermediate-Scale Quantum (NISQ) devices.

- **Ansatz:** We used a **TwoLocal** ansatz (Hardware Efficient), consisting of layers of R_y rotation gates (parameterized) and CZ entangling gates.
- **Optimizer:** We used the **COBYLA** (Constrained Optimization BY Linear Approximation) optimizer, which is gradient-free and robust to noise.
- **Objective:** Minimize the expectation value $E(\theta) = \langle\psi(\theta)|H|\psi(\theta)\rangle$.

3.2.3 Algorithm 2: Trotterization

To simulate time evolution, we used the Lie-Trotter product formula. Since the atomic term H_A and interaction term H_B do not commute ($[H_A, H_B] \neq 0$), we cannot simply exponentiate the sum. Instead, we discretize time into small steps Δt:

$$U(t) = e^{-i(H_A+H_B)t} \approx \left(e^{-iH_A\Delta t}e^{-iH_B\Delta t}\right)^M \tag{11}$$

where M is the number of Trotter steps (**reps**). Increasing M improves accuracy but increases circuit depth (and thus noise). For our hardware runs, we set $M = 5$ as an optimal trade-off.

4 Results and Analysis

4.1 Spectral Analysis: The Bloch-Siegert Shift

We first compared the energy spectra of the two models by sweeping the coupling strength g from 0 to 1.5ω.

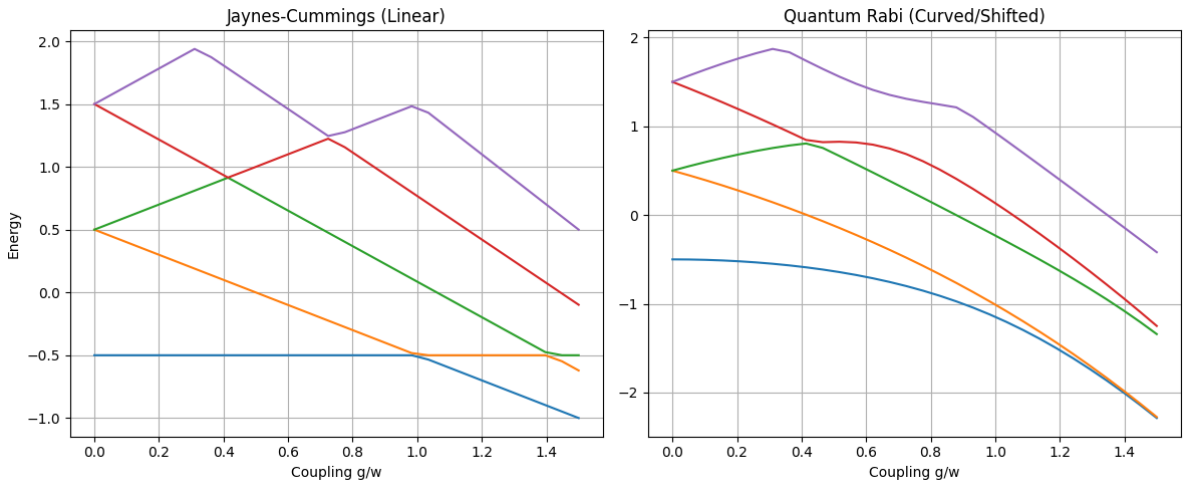

Figure 1: Energy spectrum of the JC model (Left) vs. Quantum Rabi Model (Right) as a function of coupling strength g/ω.

As shown in Figure 1, the JC model (Left) exhibits linear level splitting ($E \propto g$). The ground state energy (blue line) remains constant at -0.5ω regardless of coupling strength, because the RWA decouples the vacuum state.

In contrast, the Rabi model (Right) displays non-linear curvature. The ground state energy decreases as coupling increases, bending downwards. This curvature is the **Bloch-Siegert Shift**. It visually confirms that in the DSC regime, the atom is binding with the vacuum fluctuations, lowering the total energy of the system.

4.2 Dynamical Analysis: Collapse and Revival

We simulated the time evolution of an initially excited atom $|e, 0\rangle$ under the condition $g = \omega$ (Deep Strong Coupling).

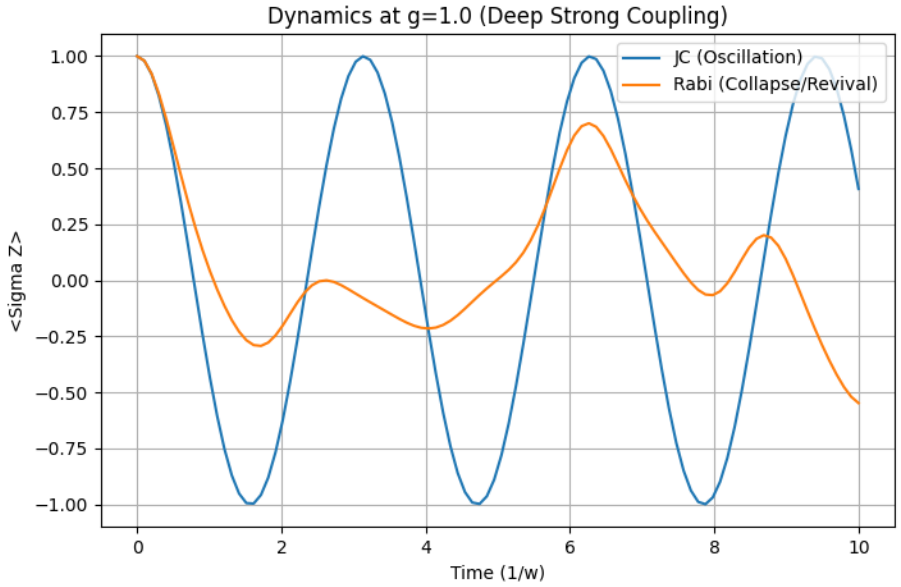

Figure 2: Time evolution of the atomic population $\langle \sigma_z \rangle$ at $g = \omega$.

Figure 2 reveals a striking difference in dynamics:

- The **Blue Line (JC)** shows standard vacuum Rabi oscillations. The atom exchanges a photon with the cavity in a coherent, periodic manner ($|e,0\rangle \leftrightarrow |g,1\rangle$). The amplitude is constant because the system is confined to a 2-dimensional subspace.
- The **Orange Line (Rabi)** shows a chaotic "Collapse and Revival" pattern. The oscillation amplitude decays to near zero (Collapse) and then re-emerges (Revival). This occurs because the counter-rotating terms open transitions to higher photon states ($|e,0\rangle \to |g,1\rangle, |e,2\rangle \dots$). The wavefunction spreads out across these multiple states in the parity chain. Since these states have incommensurate frequencies, their phases destructively interfere (collapse) and later constructively interfere (revival) [2].

4.3 Verification with VQE

To confirm our quantum mapping, we used VQE to compute the ground state energy on a simulator.

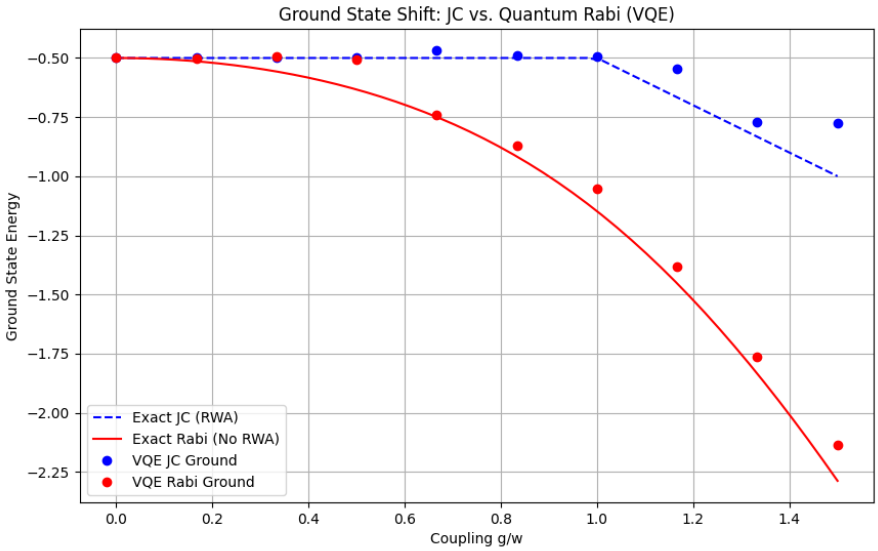

Figure 3: VQE calculation of the ground state energy. Blue Dots: JC Model. Red Dots: Rabi Model.

Figure 3 demonstrates that the VQE algorithm (Red Dots) successfully tracks the curved ground state of the Rabi model, distinguishing it from the linear JC model (Blue Dots). The match between the VQE points and the classical theory line confirms that the variational circuit can accurately represent the entangled ground state of the DSC regime.

4.4 Hardware Execution on IBM Torino

We executed the digital simulation on the **IBM Torino** superconducting quantum processor. To ensure the circuit depth fit within the coherence time of the device, we used

a truncated 2-qubit model ($N = 2$) and 5 Trotter steps.

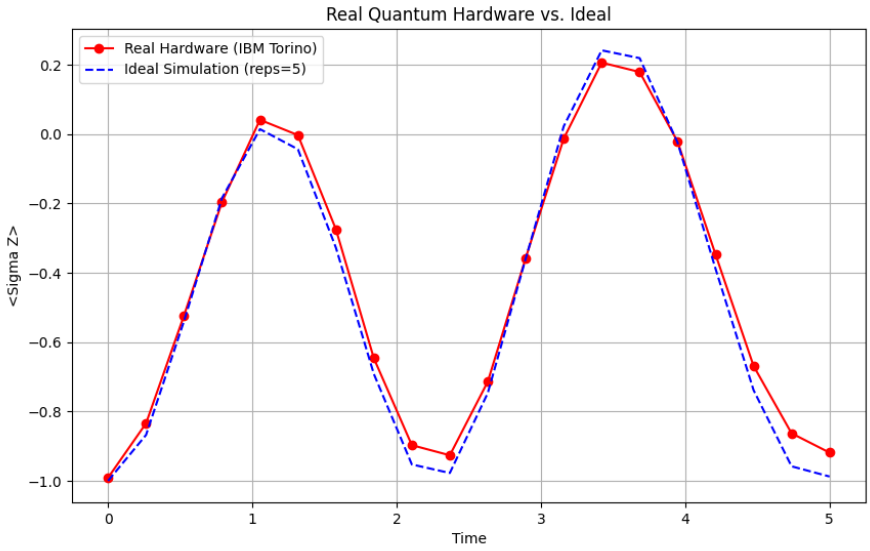

Figure 4: Experimental results from IBM Quantum hardware (Red) compared to ideal simulation (Blue).

Figure 4 shows the experimental results.

- The **Red Line** (Hardware) tracks the **Blue Line** (Ideal) with high fidelity for the first few oscillations. This confirms that the quantum processor successfully implemented the Trotterized Hamiltonian and the Rabi dynamics.
- However, a discrepancy appears at later times ($t > 4.0$). The amplitude of the hardware result is damped compared to the ideal simulation. The peak at $t = 5$ reaches only ≈ 0.9 instead of 1.0. This indicates **signal degradation** in the physical qubits due to environmental noise.

4.5 Noise Analysis and Characterization

To identify the source of the degradation seen in Figure 4, we constructed a custom noise model using `Qiskit Aer`. We tested various error channels (thermal relaxation, readout error, depolarizing error) to see which best reproduced the experimental data.

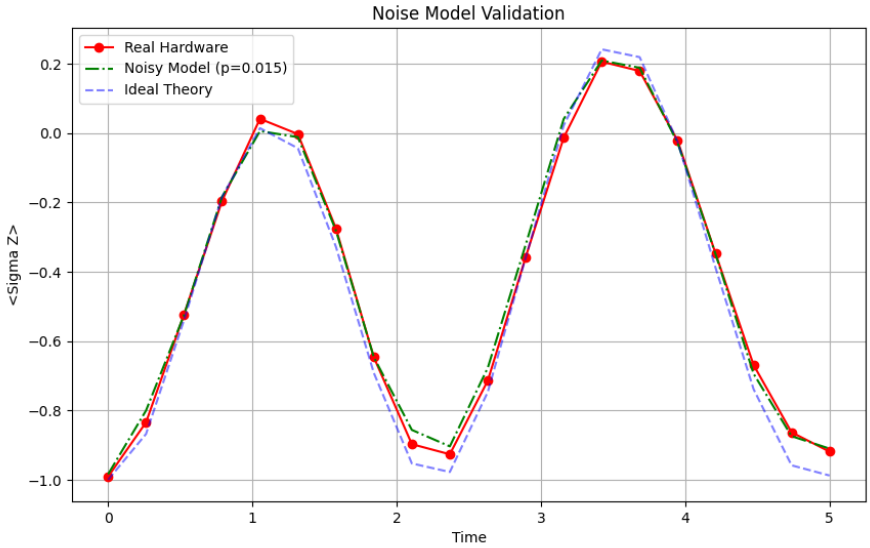

Figure 5: Comparison of Real Hardware data with a simulation including Depolarizing Noise.

As shown in Figure 5, a simulation with a **1.5% depolarizing error** injected per gate (Green Line) produces a decay profile that almost perfectly matches the real hardware (Red Line). This strong agreement suggests that the primary limitation in our experiment was gate infidelity and decoherence (T_1/T_2 relaxation), rather than algorithmic Trotter error.

5 Conclusion

In this project, we have successfully simulated the physics of the Deep Strong Coupling regime, bridging the gap between quantum optics and quantum field theory.

Our key achievements are:

1. We theoretically verified the breakdown of the Rotating Wave Approximation by calculating the exact energy spectrum, identifying the **Bloch-Siegert Shift** as a key signature of vacuum interactions.

2. We observed **Collapse and Revival** dynamics in our simulations, demonstrating the scattering of the wavefunction across the parity chains of the Hilbert space.

3. We implemented the Quantum Rabi Model on a digital quantum computer using VQE and Trotterization. Our VQE results accurately tracked the spectral shift, validating our Hamiltonian mapping.

4. We successfully executed the simulation on the **IBM Torino** quantum processor. While the hardware results matched theory initially, we observed signal degradation over time. Through noise modeling, we quantified this degradation as being consistent with a 1.5% gate error rate.

These results demonstrate the power of current NISQ (Noisy Intermediate-Scale Quantum) devices to simulate complex physical regimes that are difficult to access in standard

laboratory experiments. Future work could involve using error mitigation techniques (such as Zero-Noise Extrapolation) to extend the simulation time and circuit depth, allowing for the observation of higher-order interference effects on real hardware.

References

[1] E. T. Jaynes and F. W. Cummings, *Comparison of quantum and semiclassical radiation theories with application to the beam maser*, Proc. IEEE 51, 89 (1963).

[2] J. Casanova, G. Romero, I. Lizuain, J. J. García-Ripoll, and E. Solano, *Deep Strong Coupling Regime of the Jaynes-Cummings Model*, Phys. Rev. Lett. 105, 263603 (2010).

[3] D. Ballester, G. Romero, J. J. García-Ripoll, F. Deppe, and E. Solano, *Quantum Simulation of the Ultrastrong-Coupling Dynamics in Circuit QED*, Phys. Rev. X 2, 021007 (2012).

[4] J. Braumüller et al., *Analog quantum simulation of the Rabi model in the ultra-strong coupling regime*, Nat. Commun. 8, 779 (2017).

[5] D. Lv et al., *Quantum Simulation of the Quantum Rabi Model in a Trapped Ion*, Phys. Rev. X 8, 021027 (2018).